A Local Glutamate-Glutamine Cycle Sustains Synaptic Excitatory Transmitter Release

Hiroaki Tani,[1,*] Chris G. Dulla,[2] Zoya Farzampour,[1,3] Amaro Taylor-Weiner,[2] John R. Huguenard,[1,3] and Richard J. Reimer[1,3,4,*]

[1]Department of Neurology and Neurological Sciences, Stanford University School of Medicine, Stanford, CA 94305, USA
[2]Department of Neuroscience, Tufts University School of Medicine, Boston, MA 02111, USA
[3]Graduate Program in Neuroscience, Stanford University School of Medicine, Stanford, CA 94305, USA
[4]Neurology Service, Veterans Affairs Palo Alto Health Care System, Palo Alto, CA 94304, USA
*Correspondence: hirotaniwork@gmail.com (H.T.), rjreimer@stanford.edu (R.J.R.)
http://dx.doi.org/10.1016/j.neuron.2013.12.026

SUMMARY

Biochemical studies suggest that excitatory neurons are metabolically coupled with astrocytes to generate glutamate for release. However, the extent to which glutamatergic neurotransmission depends on this process remains controversial because direct electrophysiological evidence is lacking. The distance between cell bodies and axon terminals predicts that glutamine-glutamate cycle is synaptically localized. Hence, we investigated isolated nerve terminals in brain slices by transecting hippocampal Schaffer collaterals and cortical layer I axons. Stimulating with alternating periods of high frequency (20 Hz) and rest (0.2 Hz), we identified an activity-dependent reduction in synaptic efficacy that correlated with reduced glutamate release. This was enhanced by inhibition of astrocytic glutamine synthetase and reversed or prevented by exogenous glutamine. Importantly, this activity dependence was also revealed with an in-vivo-derived natural stimulus both at network and cellular levels. These data provide direct electrophysiological evidence that an astrocyte-dependent glutamate-glutamine cycle is required to maintain active neurotransmission at excitatory terminals.

INTRODUCTION

Synaptic transmission requires a continuous supply of neurotransmitter for release. Although most types of neurons use direct reuptake to recycle released neurotransmitters, evidence indicates that glutamatergic synapses rely predominantly on astrocytes for generation and recycling of glutamate (Hertz, 1979). Biochemical studies demonstrate that astrocytes take up glutamate and convert it to glutamine, which is released into the extracellular space and taken up by neurons as a glutamate precursor in what is known as the glutamate-glutamine cycle. The cycle is generated by a segregated expression pattern for key molecular components. Astrocytes express high-affinity

excitatory amino acid transporters that clear released glutamate from the synapse, along with glutamine synthetase (GS) that converts glutamate to glutamine, and transporters that release glutamine into the extracellular space. In a reciprocal fashion, neurons express transporters that mediate uptake of glutamine, phosphate-activated glutaminase that converts glutamine back to glutamate, and the machinery necessary for packaging and releasing glutamate through vesicle exocytosis (Danbolt, 2001). This model of cellular cooperation and compartmentalization predicts that efficacy at glutamatergic synapses is coupled to both astrocytic and neuronal metabolism. However, attempts to define a role for the glutamate-glutamine cycle in regulating excitatory synaptic transmission with standard electrophysiological analysis have met with limited success (Kam and Nicoll, 2007; Masson et al., 2006). In fact, a requirement for the cycle has only been demonstrated during epileptiform activity, a disease setting in which glutamate release is greatly increased (Bacci et al., 2002; Otsuki et al., 2005; Tani et al., 2010).

Studies in living animals have demonstrated that ~70% of synaptic glutamate is derived from the glutamate-glutamine cycle (Kvamme, 1998; Lieth et al., 2001; Rothman et al., 2003; Sibson et al., 2001). How can these in vivo studies be reconciled with electrophysiological analyses of isolated brain slices that suggest that glutamatergic neurotransmission can be sustained in the absence of the glutamate-glutamine cycle (Kam and Nicoll, 2007; Masson et al., 2006)? We reasoned that the lack of direct evidence for its requirement reflects the absence of an appropriate system in which to test this. For excitatory neurons with long axonal projections, the physical distance between the neuronal cell body and the presynaptic terminal limits the contribution of somatic sources to the pool of glutamate available for synaptic release. This suggests that a perisynaptic localization of the glutamate-glutamine cycle would be required for maintaining high-frequency neurotransmitter release from these neurons. We therefore investigated glutamate release from isolated nerve terminals by taking advantage of the anatomy of two well-defined projection neuron tracts in the hippocampus and the cortex. By acutely transecting the axons, we separated excitatory nerve terminals from their cell bodies while retaining the relationship of presynaptic structures with postsynaptic neurons and surrounding astrocytes. We found that these isolated terminals provide a reliable system for electrophysiological analysis of the role of the glutamate-glutamine cycle in excitatory

neurotransmission. During moderate activity, we found that glutamate release could be sustained in the absence of the glutamate-glutamine cycle, but not indefinitely, suggesting that there is a reservoir of glutamate and/or glutamine. Using a stimulation paradigm with alternating periods of robust activity and rest, we identified an activity-dependent reduction in synaptic efficacy that correlated with a reduction in glutamate release. The reduced efficacy was greater with inhibition of astrocytic GS and fully reversed or prevented by addition of glutamate. Surprisingly, the rate of recovery did not differ in untransected slices, suggesting that in an intact brain, a local glutamate-glutamine cycle is the predominant pathway for excitatory neurotransmitter recycling. Furthermore, natural stimulation patterns derived from in vivo recordings resulted in a similar glutamine-responsive activity-dependent reduction in synaptic efficacy. This was observed at the level of individual synapses with minimal stimulation while recording intracellularly from CA1 neurons. Together, these findings demonstrate a role for a synaptically localized glutamate-glutamine cycle in maintaining excitatory neurotransmitter synthesis and vesicle release during periods of robust activity.

RESULTS

To study the role of the glutamate-glutamine cycle in the release of neurotransmitter from axotomized terminals, we first focused on the Schaffer collateral pathway in the hippocampus. Synapses of the Schaffer collateral pathway are among the most extensively studied in the mammalian brain, and the well-delineated structure of the hippocampus permits simple isolation of the presynaptic Schaffer collateral axons from their CA3 cell bodies while retaining the structural relationship of the presynaptic bouton with the postsynaptic structures and perisynaptic astrocytes. Furthermore, bursts of 20–30 Hz activity lasting more than a minute have been observed in the mouse hippocampus during novel environment exploration (Berke et al., 2008). Thus, Schaffer collateral fibers release and must recycle or synthesize large amounts of glutamate to sustain such activities. Studies in vitro have also demonstrated that stimulation of Schaffer collateral fibers at 20 Hz drives excitatory neurotransmission at a maximal rate and exhausts the readily releasable pool of vesicles in ~3 s (Dobrunz and Stevens, 1997; Garcia-Perez et al., 2008; Stevens and Wesseling, 1999; Wesseling and Lo, 2002). Beyond this time point, a steady state of vesicle recycling is established, and the rate of neurotransmitter replenishment can define the sustained rate of release. With addition of N-methyl-D-aspartate (NMDA) receptor antagonists to block long-lasting plasticity, this experimental system allows for a direct electrophysiological analysis of the role of neurotransmitter synthesis in excitatory neurotransmission.

In hippocampal slices with Schaffer collateral fibers transected and perfused with standard artificial cerebrospinal fluid (aCSF), we established a stable baseline of evoked field excitatory postsynaptic potentials (fEPSPs) in the stratum radiatum with 0.2 Hz stimulation. A baseline was typically obtained within 10–15 min, and the fEPSPs remained stable for more than 60 min (Figure 1A, left panel). To test whether the capacity to release glutamate for extended periods of time depends upon the gluta-

mate-glutamine cycle, we preincubated slices with methionine sulfoximine (MSO), an irreversible inhibitor of the astrocytic enzyme GS. GS is required for both the glutamate-glutamine cycle and synthesis of glutamine derived de novo through anaplerosis (Schousboe et al., 1993). With a stimulation frequency of 0.2 Hz, the fEPSPs in the MSO-pretreated slices remained stable for 60 min (Figure 1A, right panel), consistent with previous findings (Kam and Nicoll, 2007; Masson et al., 2006). However, with the stimulation frequency increased to 2 Hz, after about 1,000 stimuli, there was a progressive reduction in fEPSP amplitudes in MSO-treated slices (Figure 1B, black trace). To confirm that this effect was due to inhibition of GS, we added 500 μM glutamine, a concentration in the physiological range (Moore et al., 1978). This mitigated the effect of MSO (Figure 1B, green trace and right panels), indicating that there is a reservoir of glutamate and/or metabolic precursors that can sustain activity during prolonged periods of low-frequency activity but can be depleted by periods of more robust activity.

The experiments with MSO-treated slices indicated that the glutamate-glutamine cycle is necessary for sustained excitatory neurotransmission during prolonged periods of activity. We wondered whether the demand on an intact glutamate-glutamine cycle might be exceeded by its capacity during robust activity. Assaying slices not treated with MSO and increasing the stimulation rate to 20 Hz, we found that the fEPSP amplitudes initially increased and then rapidly decreased to the point of being nearly undetectable (Figure 1C, black tracing). If this was due to loss of glutamate and/or its metabolic precursor glutamine in the effluate, then supplementation with glutamine should attenuate the loss of synaptic transmission. With addition of 500 μM glutamine, the initial increases and decreases in fEPSP amplitudes were similar to those in control slices during the first ~1,000 pulses (50 s), but after that, the relative fEPSP amplitudes were greater than those in control slices and remained stable for the duration of the experiment (Figure 1C, green tracing). This indicates that, in the presence of glutamine, synaptic transmission at isolated Schaffer collateral terminals can be maintained during prolonged periods of high-frequency stimulation.

The rapid decline in postsynaptic responses seen with 20 Hz stimulation in the presence of glutamine likely reflects high-frequency-induced short-term synaptic depression caused by a limited availability of release-ready vesicles (Dobrunz and Stevens, 1997; Sara et al., 2002; Stevens and Wesseling, 1999). We reasoned that a pattern of high-frequency stimulation alternating with periods of low-frequency stimulation might allow readily releasable vesicle pools to be replenished without necessarily allowing neurotransmitter levels to recover fully. This could lead to more neurotransmitter release over time and place a greater demand on glutamate supply sources. Therefore, we used a stimulation protocol interleaving high-frequency stimuli (HFS; 20 Hz) for 50 s (1,000 pulses) with low-frequency stimuli (LFS; 0.2 Hz) for 200 s (40 pulses), hereafter referred to as intermittent high-frequency stimulation (iHFS) protocol. We chose 50 s for the HFS interval both because this is the point at which we started to see an effect with glutamine in the continuous HFS paradigm, and because this is within the range of physiological bursts of high-frequency activity in the hippocampus (Berke et al., 2008). With the iHFS protocol, we are also able to
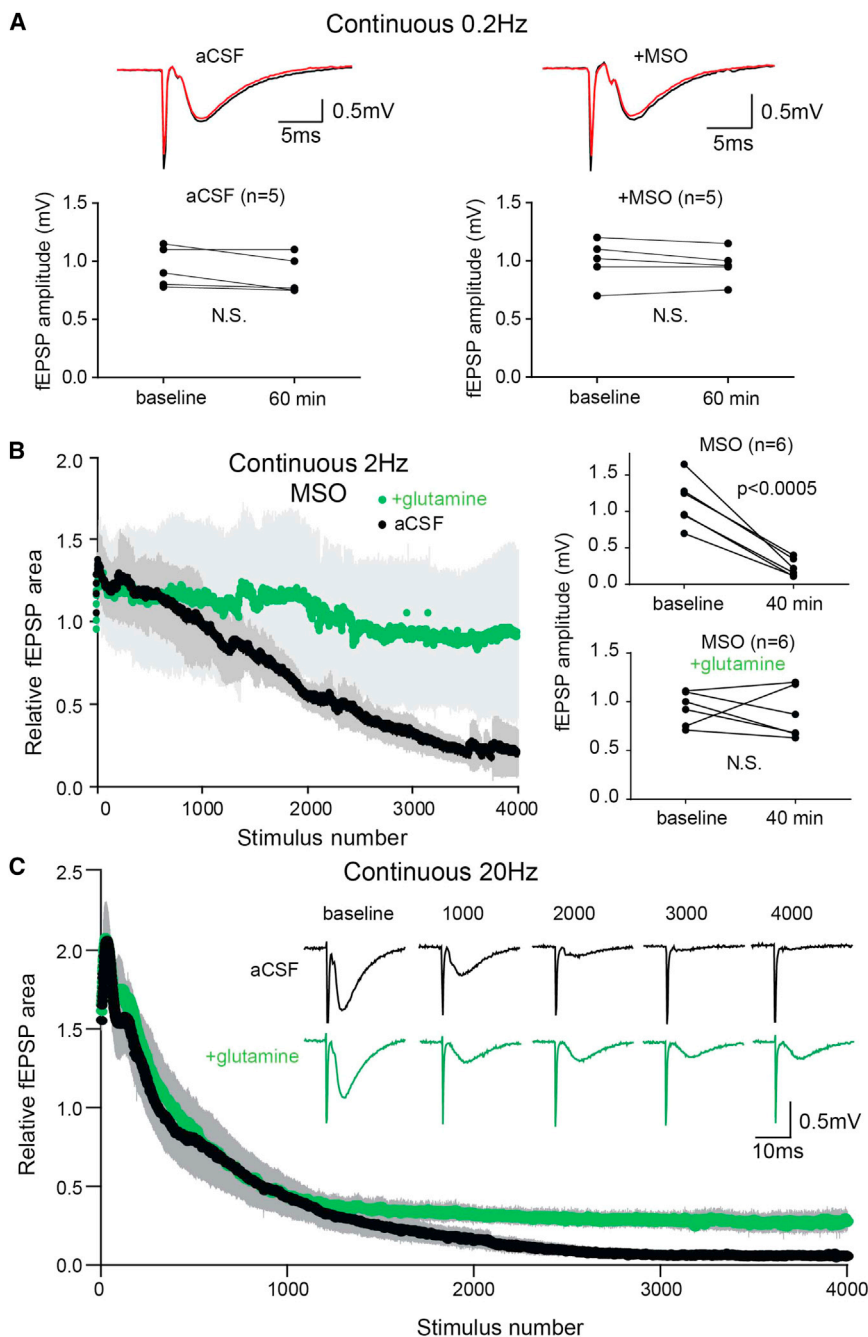
Figure 1. Glutamine Prevents fEPSP Depression during High-Frequency Repetitive Stimulation of the Schaffer Collaterals

(A) Example traces at baseline (black) and after 60 min (red) of continuous 0.2 Hz stimulation (upper) and paired plot of fEPSP amplitudes (lower) for untreated slices (left) and slices pretreated with MSO to inhibit GS (right). N.S., not significant.

(B) Time course of relative fEPSP area during continuous 2 Hz stimulation (4,000 stimuli; 33.3 min) of the Schaffer collaterals (left panel) in slices treated with MSO in aCSF (black; n = 6) and with addition of 500 μM glutamine (green; n = 6). Evoked fEPSP amplitudes during 0.2 Hz stimulation at baseline and at 40 min (~6 min after 2 Hz stimulation) show significant fEPSP depression (Student's t test, p < 0.0005) in MSO-treated slices, but not in glutamine (right panel).
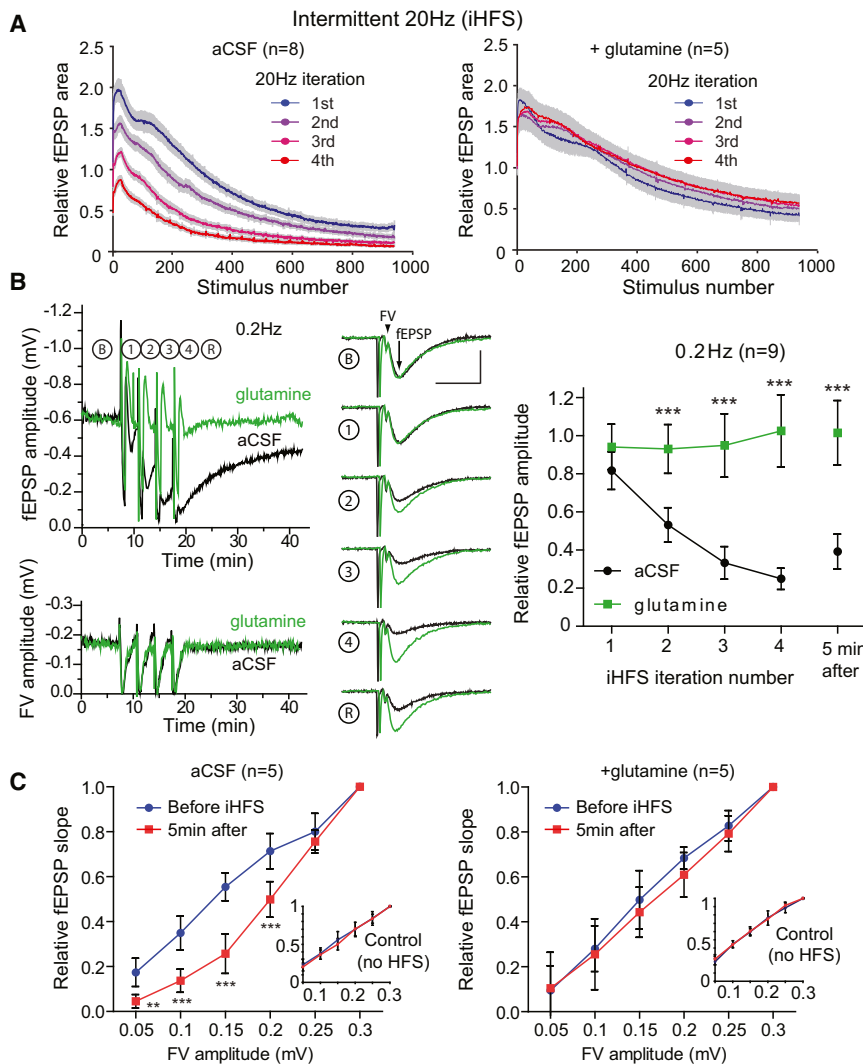
(C) Time course of continuous 20 Hz stimulation of Schaffer collaterals in aCSF (black; n = 6) and with glutamine (green, n = 4). Inset shows example traces at indicated stimulus numbers. Gray bars indicate SEM.

cumulative glutamine-sensitive reduction in fEPSPs with iHFS that persisted for more than 5 min after termination of the final 20 Hz iteration (Figure 2B, left panel upper tracings and right panel). In the glutamine-treated slices, the fEPSPs rapidly recovered to baseline at 0.2 Hz after HFSs. This suggests that vesicle pools are replenished quickly during LFS and that in the absence of glutamine, the incomplete recovery was due to depletion of glutamate available for neurotransmission. Interestingly, the reduction in fEPSP amplitudes with iHFS and subsequent recovery during low-frequency stimulation were similar in transected and intact hippocampal slices (Figure S1 available online). The fEPSP amplitudes remained reduced by more than half in both groups even 5 min after iHFS was completed.

Although we suspected that limited neurotransmitter supply was the primary

analyze synaptic activity during the periods of LFS, without confounding factors associated with high-frequency stimulation such as changes in releasable vesicle pool size (Dobrunz and Stevens, 1997; Sara et al., 2002; Stevens and Wesseling, 1999). With iHFS, we again found a decrease in the evoked fEPSP amplitudes during 20 Hz stimulation but also a further progressive decrease with subsequent HFS iterations (Figure 2A, left panel). When slices were treated with glutamine, there was also a decrease in the fEPSP amplitudes during 20 Hz stimulation train but full recovery between HFS iterations (Figure 2A, right panel). The time course of fEPSPs demonstrates a robust

cause for the reduced fEPSPs after prolonged high-frequency activity, another possible explanation was that the efficacy with which electrical stimulation elicited an action potential waned. To determine whether this contributed to the reduced synaptic signaling, we examined fiber volleys (FVs) during the periods of 0.2 Hz stimulation. Aside from transient suppression during HFSs, FVs were stable over the course of the experiment and were not affected by glutamine (Figure 2B, left panel lower tracings; Figure S2), indicating that there were no long-term changes in intrinsic excitability of the stimulated fibers by iHFS or by glutamine.

Figure 2. iHFS Causes Use-Dependent fEPSP Depression that Is Prevented by Glutamine

(A) Evoked fEPSP amplitudes during intermittent 20 Hz stimulation with four iterations of 1,000 pulses at 20 Hz separated by 200 s of recovery at 0.2 Hz in aCSF (left panel; n = 8) and aCSF with 500 μM glutamine (right panel; n = 5). Gray bars indicate SEM.

(B) Time course of fEPSP amplitude (upper left) and FV amplitude (lower left) during iHFS protocol on slices in aCSF (black) and aCSF with glutamine (green). Traces of evoked fEPSP during 0.2 Hz stimulation at baseline (B), after successive iterations of 1,000 pulses at 20 Hz (1–4), and after a subsequent 5 min recovery period (R) of 0.2 Hz stimulation (middle panel) and summary (right panel; n = 9, two-way repeated-measures ANOVA with Bonferroni posttest, ***p < 0.001; error bars represent 95% CI) demonstrate activity-dependent reduction in fEPSP amplitude. FV and fEPSP are indicated by the arrowhead and arrow, respectively, in baseline sample tracings in (B). Scale bars, 10 ms and 0.5 mV (middle panel).

(C) Graphs of input (FV amplitude in mV) and output (relative fEPSP slope) are plotted for stimulated (iHFS) electrodes with control stimulation pathway (continuous 0.2 Hz stimulation) shown in insets. I/O curves before iHFS (blue) and after (red) in the absence (left) and presence (right) of glutamine are shown (two-way repeated-measures ANOVA with Bonferroni posttest, **p < 0.01 and ***p < 0.001; error bars represent 95% CI). The same recording electrode was used for iHFS and control-stimulating electrodes.

We next sought to ensure that the glutamine-responsive reduction in fEPSP amplitude did not reflect diffuse metabolic changes in the slice. To assess this, we compared input-output (I/O) curves from two laterally displaced stimulating electrodes, with one site stimulated as above with the iHFS protocol and the other (control) assessed continuously at 0.2 Hz, while recording from a single central recording electrode. With the iHFS protocol, there was a significant depression (rightward shift) of the I/O curve, especially for small-to-moderate FV amplitudes. This shift was not noted for the control electrode (Figure 2C, left panel) or for either electrode with slices incubated with glutamine (Figure 2C, right panel), suggesting that the effects of iHFS and glutamine are limited to the synapses that have been activated.

To determine how long this effect of high-frequency activity on synaptic efficacy would last, we monitored fEPSPs during an extended recovery period. We found that after the iHFS protocol in aCSF, there was a slow recovery of fEPSP amplitudes that was still incomplete after 20 min (Figures 3A and 3B). With subsequent addition of glutamine, the recovery of fEPSP amplitude

appeared to be hastened and near complete within 20 min. We next compared recovery during an extended LFS period after completion of iHFS without and with glutamine. Without glutamine, there was little increase in the average relative fEPSP amplitude between 30 and 60 min after iHFS (0.53 ± 0.30 and 0.59 ± 0.29, respectively; p = 0.239, paired two-tailed t test). There was, however, a significant recovery when glutamine was added at the start of the extended LFS period (0.58 ± 0.22 and 0.82 ± 0.34, respectively; p = 0.0128, paired two-tailed t test). The addition of glutamine did not affect the FV but caused normalization of the I/O curve (Figure 3C), consistent with its specific effect on the stimulated pathway.

The extent to which endogenous glutamine synthesized by astrocytes is required for the sustained periods of high-frequency excitatory synaptic transmission in our system is unclear, but the reduction in synaptic efficacy caused by the gliotoxins fluoroacetate and fluorocitrate suggests that astrocytes are required for the maintenance of excitatory neurotransmission (Bacci et al., 2002; Bonansco et al., 2011; Keyser and Pellmar, 1994). To test this, we preincubated slices with MSO to inhibit the astrocytic enzyme GS. We expected that MSO would cause a more rapid reduction in fEPSP amplitude and that this effect would be attenuated by the addition of glutamine. We found
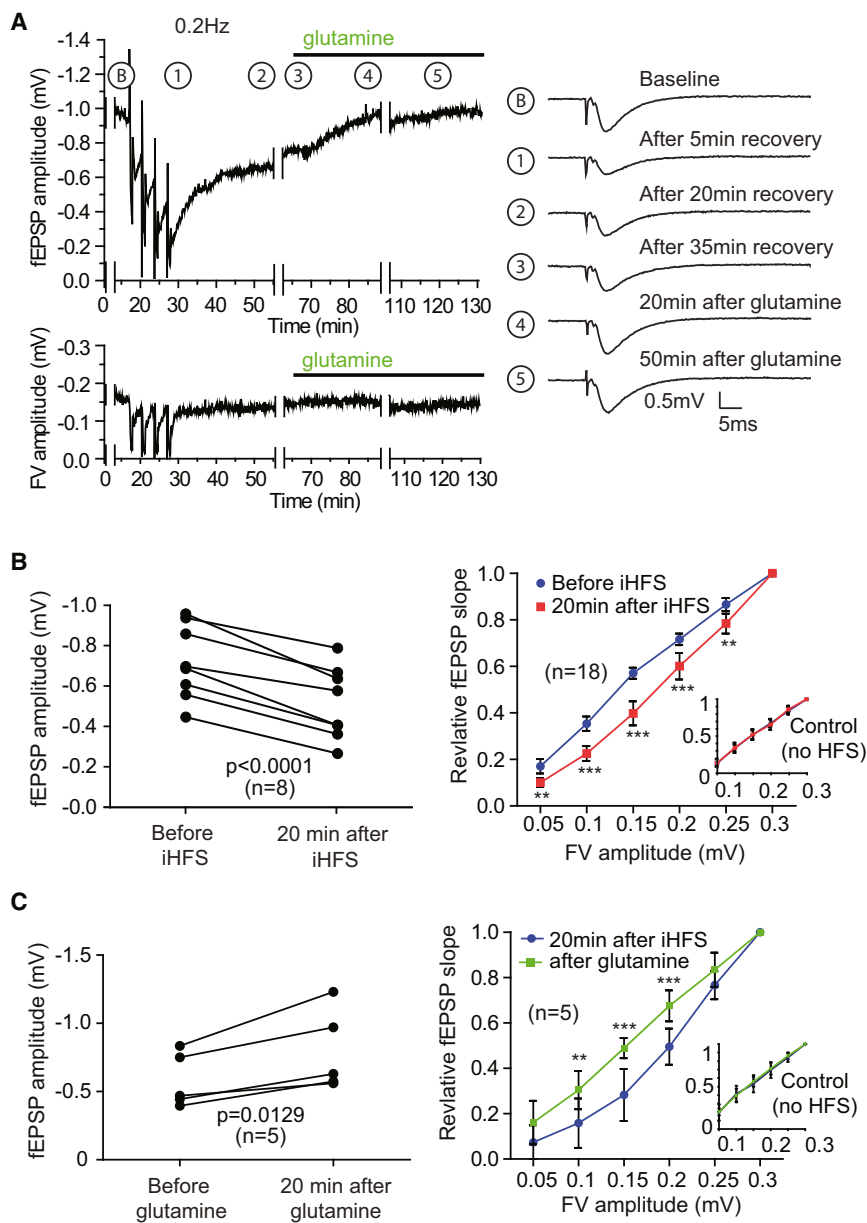
Figure 3. Glutamine Reverses iHFS-Induced fEPSP Amplitude Reduction

(A) Time course of fEPSP amplitude (upper trace) and FV (lower trace) with standard iHFS protocol followed by addition of glutamine. Traces during collection of data for I/O relationship were removed (and depicted by gaps) for clarity. Example traces during 0.2 Hz stimulation at indicated time points are depicted on right.

(B) Paired plot of fEPSP amplitude measurement before and after iHFS protocol (left panel) shows significant depression at 20 min after the iHFS (Student's t test, p < 0.0001) and a corresponding rightward shift in the I/O curve (right panel). There is no change in the I/O curve for the control pathway (inset). Error bars represent 95% CI.
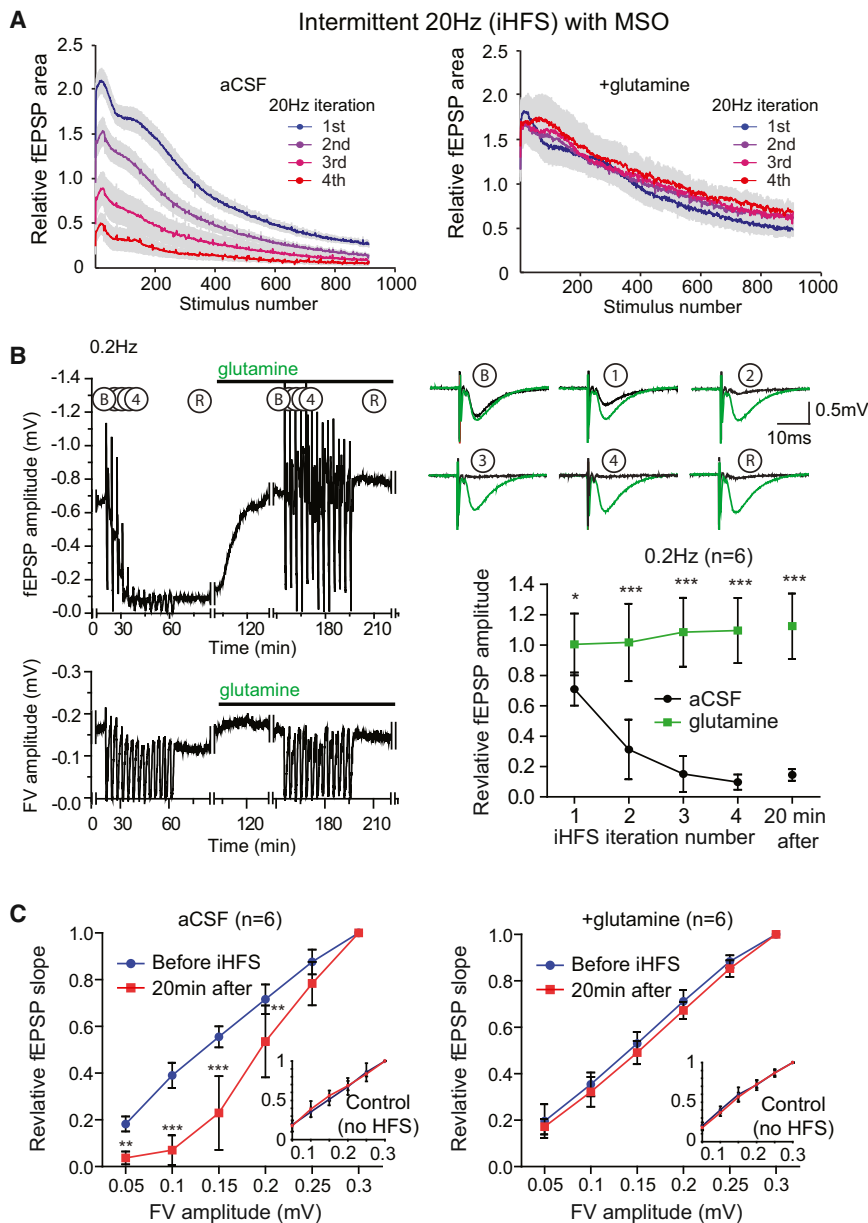
(C) Addition of glutamine 20 min after iHFS protocol significantly increases fEPSP amplitude 20 min later (left panel; Student's t test, p = 0.0129). There is also a corresponding leftward shift of the I/O curve (right panel). Note that glutamine does not affect the I/O curve of the control pathway (inset). For statistical analyses of the I/O curves, two-way repeated-measures ANOVA with Bonferroni post-test was applied (**p < 0.01 and ***p < 0.001). Error bars represent 95% CI.

tudes and normalization of I/O curves, again with no discernable difference with slices to which glutamine was added (cf. Figures 4B and 4C to Figures 2B and 2C). The effect of MSO and its reversal with glutamine support the hypothesis that astrocyte-derived glutamine is required for maintaining synaptic transmission during prolonged periods of intermittent high-frequency activity.

Reductions in synaptic efficacy can occur through a number of different mechanisms, including changes in postsynaptic responsiveness (Collingridge et al., 2010). To confirm that our results reflect changes in glutamate release, we used two independent approaches. First, we used Förster resonance energy transfer (FRET)-based glutamate biosensor imaging to measure extracellular glutamate transients (Figure 5A). This biosensor is a chimeric protein composed of cyan fluorescent protein (CFP) and the yellow fluorescent protein (YFP) variant Venus inserted into the N-terminal and C-terminal regions of the bacterial glutamate binding protein YbeJ, respectively. Glutamate binding causes a conformational change in the protein, which results in a decrease in FRET efficiency between the CFP and Venus. The biosensor allows for qualitative measurement of glutamate release in brain slices throughout an optic field with temporal resolution in the millisecond scale (Dulla et al., 2008, 2012). As expected, we found a decrease in glutamate biosensor signal with evoked release following iHFS, and this was prevented by glutamine (Figure 5B). As a second approach,

that pretreatment of slices with MSO had little effect on the evoked fEPSP amplitudes during the first epoch of 20 Hz stimulation in the iHFS protocol, but with subsequent iterations, the recovery between HFS trains was much less complete than in untreated slices—ultimately, fEPSPs were abolished (Figure 4A, left panel). Even after 20 min of LFS, the fEPSP amplitudes did not recover in the MSO-treated slices (Figure 4B). With addition of glutamine to the MSO-treated slices, there was complete and persistent recovery between iterations of the high-frequency stimulation and no discernable difference between MSO-treated slices rescued with glutamine and slices to which glutamine alone was added (cf. Figure 4A right panel to Figure 2A right panel). Furthermore, when glutamine was added to MSO-treated slices after iHFS, there was a complete recovery of fEPSP ampli-

Figure 4. Inhibiting Glutamine Synthesis with MSO Enhances iHFS-Induced fEPSP Depression

(A) Evoked fEPSP amplitudes for MSO-treated slices during four iterations of 1,000 pulses at 20 Hz separated by 200 s of recovery at 0.2 Hz in aCSF (left panel; n = 8) and aCSF with 500 μM glutamine (right panel; n = 5). Gray bars indicate SEM.

(B) Representative time course of evoked fEPSPs (upper) and FVs (lower) in MSO-treated slice. Note that adding glutamine after iHFS was associated with recovery that persisted during an additional 13 HFS iterations. Gaps represent time periods during which data for the I/O relationship were being collected. Traces of evoked fEPSP during 0.2 Hz stimulation at baseline (B), after successive iterations of 1,000 pulses at 20 Hz (1–4), and after a subsequent 5 min recovery period (R) of 0.2 Hz stimulation (upper-right panel) and summary (lower-right panel; n = 6, two-way repeated-measures ANOVA with Bonferroni posttest, *p < 0.05 and ***p < 0.001; error bars represent 95% CI) demonstrate the reduction in fEPSP in the MSO-treated slices and the recovery with addition of glutamine.

(C) I/O curves before iHFS (blue) and after (red) for MSO-treated slices in the absence (left) and presence (right) of glutamine (two-way repeated-measures ANOVA with Bonferroni posttest, **p < 0.01 and ***p < 0.001; error bars represent 95% CI). Insets show I/O curves for laterally displaced control electrodes that were stimulated continuously at 0.2 Hz.

we used the competitive AMPA receptor antagonist γ-D-glutamylglycine (γ-DGG) to assess synaptic glutamate levels (Christie and Jahr, 2006; Liu et al., 1999). This low-affinity antagonist has rapid equilibration kinetics with AMPA receptors and competes with glutamate for receptor binding during the glutamate transient associated with exocytosis. As a result, lower concentrations of glutamate are more effectively blocked by γ-DGG. We found that the effect of γ-DGG was enhanced even after only two iterations of HFSs (Figure 5C). In slices pretreated with MSO, the effect of γ-DGG was again enhanced by iHFS, whereas with addition of glutamine to MSO-pretreated slices, the efficacy of γ-DGG was unchanged by iHFS (Figures 5D and 5E). Together, the findings with the biosensor and γ-DGG support the conclusion that iHFS leads to a reduction in gluta-

mate release and reduced synaptic concentrations of glutamate.

Although unfilled synaptic vesicles can undergo exocytosis, it has been suggested that presynaptic cytosolic transmitter content influences vesicle release in cholinergic (Poulain et al., 1986) and GABAergic neurons (Wang et al., 2013). Because the paired-pulse ratio depends upon the probability of release (Branco and Staras, 2009; Hanse and Gustafsson, 2001), we examined this after iHFS on MSO-pretreated slices with and without glutamine. We found an increase in paired-pulse ratio after iHFS that was prevented by addition of glutamine, suggesting that glutamine influences release probability at excitatory synapses (Figure S3).

We wondered whether the dependence on the glutamate-glutamine cycle is shared by other excitatory synapses. To test this, we established a system for electrophysiological analysis of neurotransmitter release from isolated layer I axons in the neocortex (Figure 6A) based on a previously described preparation by Cauller and Connors (1994). This allowed us to stimulate the axotomized fibers in layer I and record synaptic responses from layer III where the pyramidal cells are connected via distal apical dendrites projecting to layer I. At 0.2 Hz stimulation
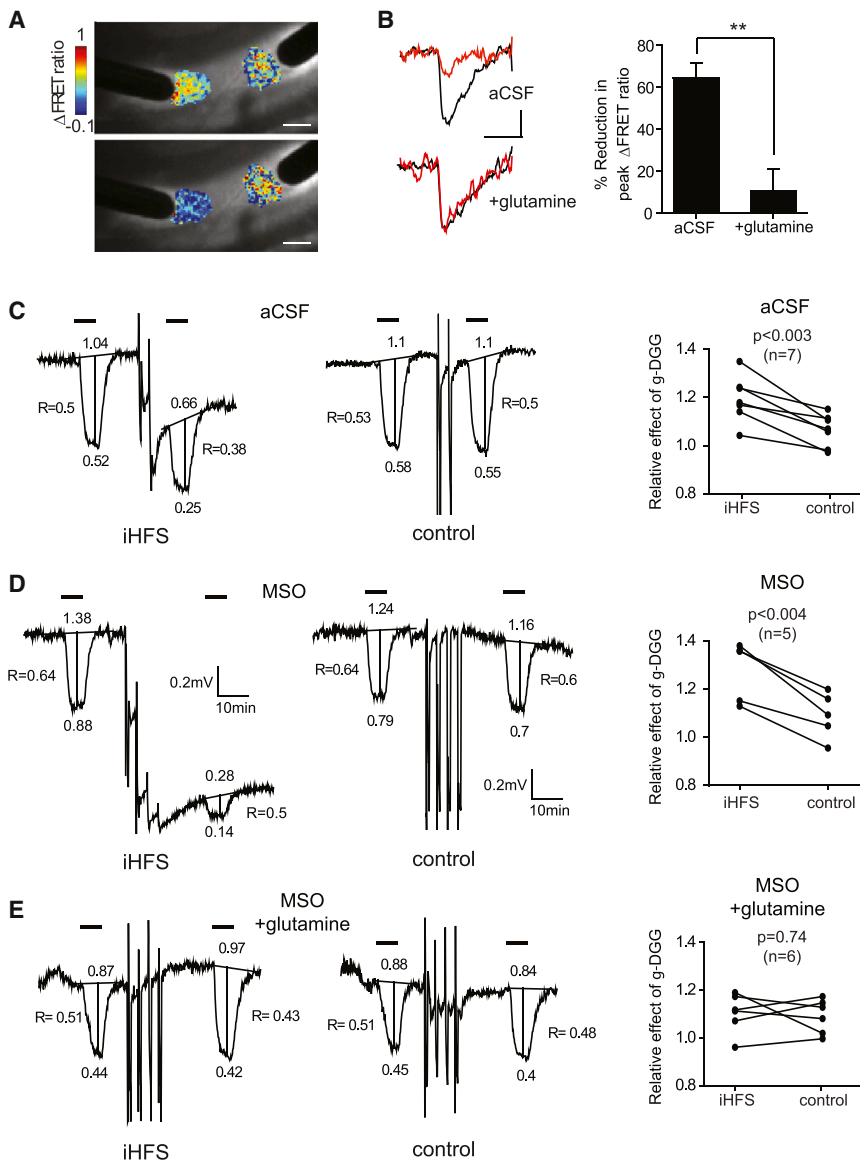
Figure 5. Reduction in Evoked Glutamate Release after iHFS Is Prevented by the Addition of Glutamine

(A) Representative heatmaps of glutamate biosensor FRET change (ΔFRET) for regions of interest adjacent to stimulating electrodes in the Schaffer collaterals overlaid on a bright-field image. Baseline signal (top panel) was obtained during an initial period of 0.2 Hz stimulation at both electrodes. After the left electrode was subjected to the iHFS protocol (bottom panel), there was a marked decrease in the signal, whereas there was little change in the signal at control electrode stimulated continuously at 0.2 Hz (right electrode). Scale bars, 200 μm.

(B) Representative time course of evoked FRET signal change by iHFS electrode in aCSF (upper) and in glutamine (lower) at baseline (black) and after iHFS (red). Scale bars, 100 ms; 0.005 ΔFRET. Summary of the reduction in evoked peak ΔFRET 5 min after iHFS with and without glutamine is presented (n = 4 aCSF, n = 7 glutamine, one-way ANOVA, **p = 0.002). There were no significant differences at the control electrode stimulated with continuous 0.2 Hz in presence and absence of glutamine (data not shown). Error bars indicate SEM.

(C–E) Effect of low-affinity, fast-equilibrating AMPA receptor antagonist γ-DGG. Example traces and corresponding paired sample data (analyzed by Student's t test) show the effect of 1 mM γ-DGG applied for 6 min (indicated as black bars in traces) before and after iHFS (left traces) compared to control electrode (right traces) in the same slice in (C) aCSF, (D) MSO-pretreated slices, and (E) MSO-pretreated slices to which glutamine was added. The bottom number represents the evoked amplitude 5 min after addition of γ-DGG, and the top number represents the evoked amplitude in the absence of γ-DGG, derived from the evoked amplitudes immediately before and after γ-DGG wash-in. R is the ratio of the amplitude of γ-DGG effect to the baseline amplitude (equal to the bottom number divided by the top number). The change in effect of γ-DGG was calculated by determining the change in ratio of amplitude reduction caused by γ-DGG before and after iHFS.

frequency, we saw no reduction in the fEPSP amplitude (Figure 6B). We therefore again used the iHFS paradigm. Compared to the hippocampus, the neocortex was more resistant to the reduction in fEPSP amplitude, requiring up to 13 iterations with 20 Hz stimulation to see a substantial loss of measurable fEPSPs. As with the hippocampal preparation, the reduction in fEPSP amplitude was eliminated by addition of glutamine to the perfusate (Figure 6C) and enhanced by pretreatment with MSO (Figure 6D).

To determine whether dependence of excitatory neurotransmission on the glutamate-glutamine cycle can be elicited with naturally occurring neuronal activity, we obtained in vivo unit recordings representing firing patterns of single CA3 pyramidal cells from a freely moving rat running laps in a field (courtesy of Dr. Kenji Mizuseki, Allen Institute for Brain Science, and Dr. György Buzsaki, New York University Neuroscience Insti-

tute). We converted 12 min of continuous recording from two representative CA3 cells with low activity (natural low-frequency stimulation [nLFS], mean 0.3 Hz and peak 6 Hz) and high activity (natural high-frequency stimulation [nHFS], mean 5.4 Hz and peak 44 Hz) to time-stamped stimulus patterns to drive the stimulators simultaneously on parallel Schaffer collateral fibers. This duration was chosen because it represented approximately 4,000 pulses for nHFS (4,032), consistent with other experiments. To obtain a baseline and assess recovery, fEPSPs were evoked at 0.2 Hz before and after the natural stimulus patterns. nHFS caused almost the same extent of fEPSP run down as four iterations of iHFS, whereas there was no effect with nLFS (Figures 7A and 7B). Same-slice comparisons were made by applying the natural stimulus patterns first in aCSF then with glutamine added. We found a glutamine-responsive depression of fEPSP with nHFS, but not with nLFS (Figures 7B and 7C, top
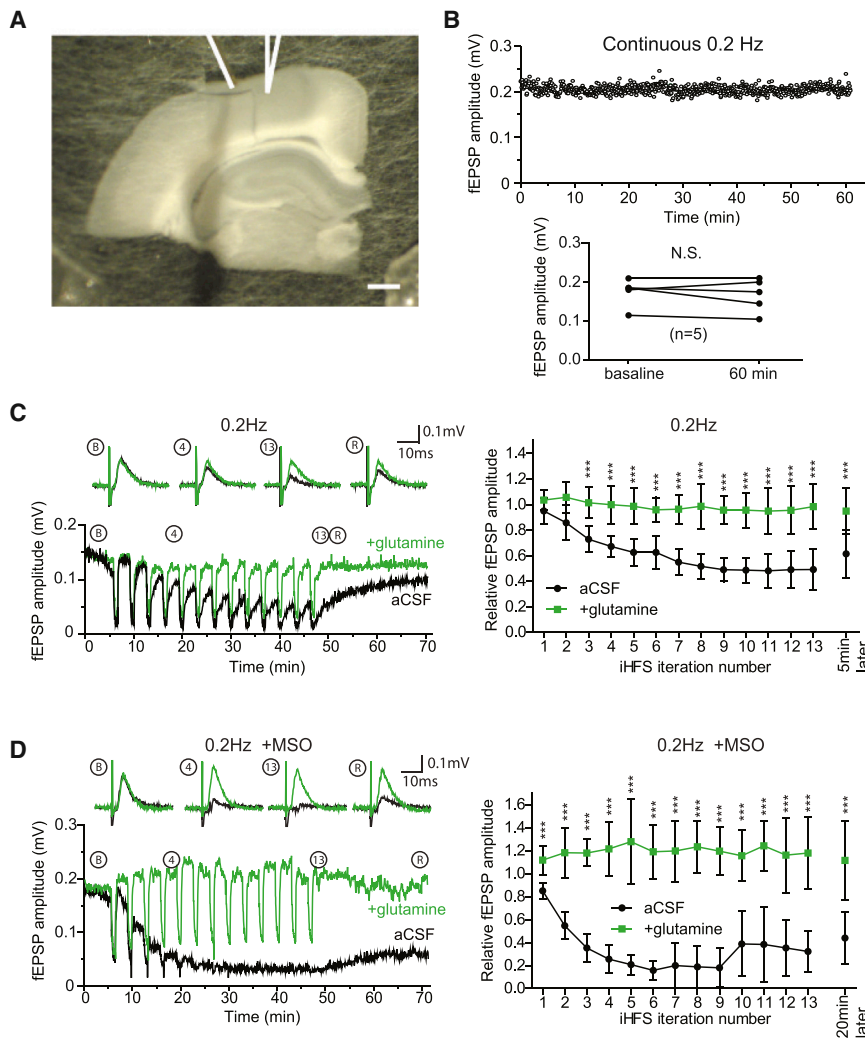
Figure 6. Glutamine Prevents fEPSP Depression during Repetitive Stimulation of Layer I Cortical Afferents

(A) Bright-field image of a rat brain slice in which layer I cortical axons have been transected and separated from on column deeper layers. Positions of stimulating (left) and recording electrode (right; in layer III where layer V apical dendrites project) are depicted by line drawings. Scale bar, 1 mm.

(B) Representative time course of evoked fEPSP amplitude during continuous 0.2 Hz stimulation protocol (upper) and plot of paired fEPSP amplitude measurements at 5 and 60 min for five slices stimulated continuously at 0.2 Hz (lower; Student's t test, no significant difference).

(C) Representative time course of evoked fEPSP amplitudes recorded during 0.2 Hz stimulation period during baseline (B), after 4th (4) and 13th (13) HFS iteration, and during recovery (R) with sample traces above (black trace indicates aCSF; green trace indicates glutamine). Summary of fEPSP amplitude after each HFS iteration is presented (right panel; n = 5, two-way repeated-measures ANOVA with Bonferroni posttest, ***p < 0.001; error bars represent 95% CI).

(D) As in (C) with slices preincubated with GS inhibitor MSO.

DISCUSSION

The glutamate-glutamine cycle is a well-established biochemical pathway, but direct evidence for its role in the synthesis of synaptically released glutamate has been lacking. Indeed, results of previous physiological studies have argued against a requirement for the cycle i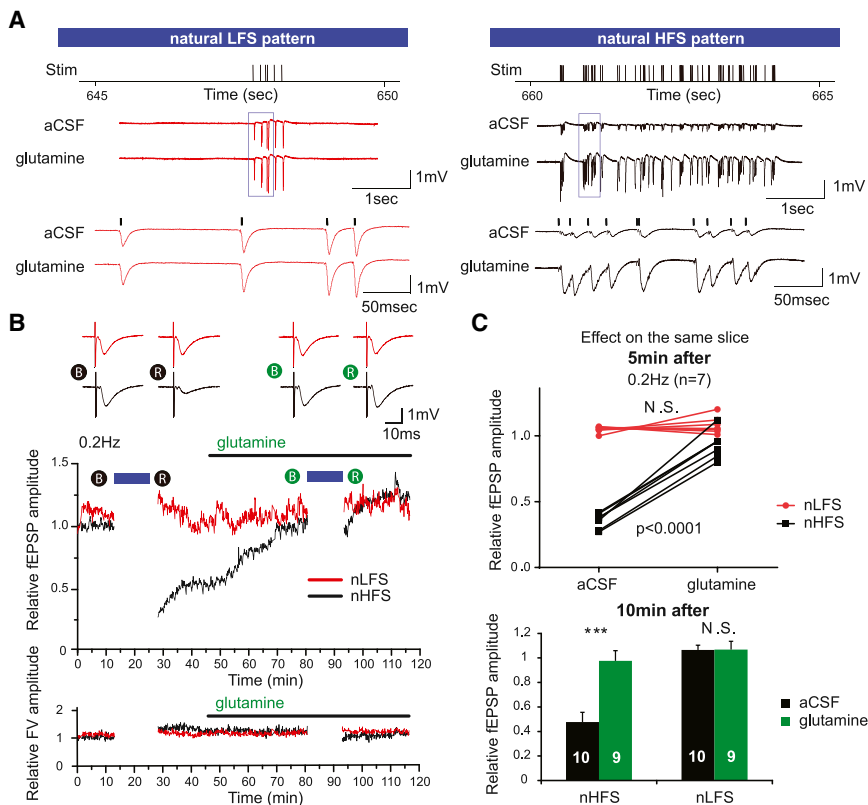n excitatory neurotransmission (Kam and Nicoll, 2007; Masson et al., 2006). Similar to these previous studies, we found that with a low-frequency stimulation protocol, glutamatergic synaptic transmission can persist for extended periods of time in the absence of a functional glutamate-glutamine cycle even from axotomized synaptic terminals. However, we found that increasing the stimulation frequency readily uncovered a requirement for the glutamate-glutamine cycle and that with both alternating periods of high-frequency and low-frequency stimulation and high-frequency natural stimulus pattern, the requirement was more apparent.

Our findings with the axotomized preparations indicate that prolonged high-frequency excitatory neurotransmission can be sustained by a local synaptic glutamate-glutamine cycle. This model of a perisynaptic intercellular metabolic pathway is supported by the subcellular expression of the molecular components of the cycle. Endfeet of astrocytes that surround synapses express the high-affinity glutamate transporters as well as the system N glutamine transporters that are involved in glutamine efflux, whereas phosphate-activated glutaminase that converts glutamine to glutamate is expressed in excitatory axons (Aoki et al., 1991; Boulland et al., 2002; Danbolt, 2001). Recently,

panels). Furthermore, amplitudes of fEPSPs 10 min after nHFS (Figure 7C, bottom panel) remained depressed in aCSF (0.478 ± 0.079) but almost completely recovered in glutamine (0.975 ± 0.084).

Finally, we evaluated the effects of neurotransmitter depletion at the synaptic level by repeating the experiments with natural stimulus patterns using minimal stimulation of Schaffer collateral fibers coupled with intracellular recordings of CA1 cells to more closely approximate in vivo CA3 neuronal activity. As with the field recordings, we established a baseline with 0.2 Hz stimulation at both electrodes, followed by 12 min during which one electrode was stimulated with the nLFS pattern and the other with the nHFS pattern. This was followed by a return to 0.2 Hz stimulation at both electrodes. Analysis of evoked EPSCs demonstrates that whereas there was no difference in evoked amplitudes after nLFS in aCSF or glutamine (Figures 8A and 8B), there was a significant reduction in minimally evoked amplitudes after nHFS in aCSF, but not in glutamine (Figures 8C and 8D). The reduction in EPSC amplitudes with nHFS in aCSF persisted for at least 10 min, consistent with our field recording results.

Figure 7. In-Vivo-Derived Natural Stimulus Pattern Reveals Glutamine-Dependent Reduction in Evoked fEPSPs

Twelve minutes of in-vivo-derived neuronal firing patterns were replayed as an nLFS or nHFS on parallel Schaffer collateral fibers in the absence or presence of glutamine.

(A) Five seconds of representative field recording traces near the end of 12 min of nLFS and nHFS show no difference between aCSF and glutamine treatment on the same slice with nLFS, but a significant depression in fEPSP amplitudes with nHFS that is prevented by glutamine. Stimulus artifacts were removed for clarity.

(B) Traces of evoked fEPSPs (upper panel) during 0.2 Hz stimulation at baseline (B) and after 5 min recovery (R) from natural stimulus patterns for slices perfused first with aCSF (black filled circles, left) and then with aCSF plus glutamine (green filled circles, right). Traces of nLFS protocol electrode are in red and those of nHFS protocol electrode in black. Sample time course of relative fEPSP amplitude (middle panel) and FV amplitude (lower panel) evoked at 0.2 Hz during baseline acquisition and after recovery from nLFS (red) and nHFS (black) protocols initially in aCSF and then with addition of glutamine is shown. Blue bars indicate duration of nLFS/nHFS.

(C) Paired analysis of evoked fEPSP amplitudes in aCSF and aCSF with glutamine 5 min after natural stimulus protocols (top) revealed no difference in evoked fEPSP amplitudes after nLFS, but fEPSP amplitude depression with nHFS in aCSF that was markedly attenuated in the presence of glutamine (n = 7, two-way repeated-measures ANOVA with Bonferroni posttest, p < 0.0001). Relative fEPSP amplitudes remained significantly depressed 10 min after nHFS in aCSF (0.478 ± 0.079; Student's t test, ***p < 0.0001) but almost completely recovered in the presence of glutamine (0.975 ± 0.084). Error bars indicate SEM.

coupling of glutamate uptake and glutamine release by astrocytes has been elegantly demonstrated by Uwechue et al. (2012). Billups and colleagues showed that uptake of glutamate released from neurons can trigger synthesis and release of glutamine from perisynaptic astrocytes (Uwechue et al., 2012). Our findings provide direct evidence for the other half of the glutamate-glutamine cycle in neurotransmitter metabolism, i.e., utilization of glutamine by neurons for synthesis of synaptically released glutamate. Interestingly, Billups and colleagues detected glutamine release by measuring electrogenic glutamine uptake into the postsynaptic MNTB neuron at the Calyx of Held (Uwechue et al., 2012). Because these neurons are GABAergic, their findings indicate that glutamine derived from synaptically released glutamate can serve as the precursor for the inhibitory neurotransmitter that modulates the excitatory network activity (Fricke et al., 2007; Liang et al., 2006). After this manuscript was submitted, Billups and colleagues have demonstrated that inducible presynaptic glutamine transport supports glutamatergic transmission at the calyx of Held synapse (Billups et al., 2013), providing further support to our results here in the cortex and hippocampus.

The attenuation of run down of fEPSPs by glutamine in both hippocampal Schaffer collateral and the neocortical layer I preparations suggests that the local synaptic glutamate-glutamine cycle may be common to excitatory synapses of projection neu-

rons throughout the mammalian CNS. The marked difference in the rates of fEPSP depression in control conditions (cf. Figures 2B and 6C), despite the similar time course for fEPSP depression in MSO (cf. Figures 4B and 6D), suggests a regional variability in the glutamate-glutamine cycle. Interestingly, the number of synapses contacted by each astrocyte is four times higher in the hippocampus than in neocortex (Bushong et al., 2002; Halassa et al., 2007), indicating that the synapse/astrocyte ratio may define the capacity of the local glutamate-glutamine cycle and the capacity for sustained high-frequency synaptic activity.

Our initial experiments, and those of others (Kam and Nicoll, 2007; Masson et al., 2006), suggest that synaptic transmission during LFS is completely independent of the cycle. Although the glutamate-glutamine cycle is the primary mechanism for recycling released glutamate (Bergles and Jahr, 1998), there is evidence for presynaptic uptake of glutamate and expression of the Na$^+$-dependent excitatory amino acid transporter GLT1 in Schaffer collaterals (Furness et al., 2008; Gundersen et al., 1993). However, the minimal recovery of fEPSPs of the MSO-treated slices following iHFS suggests that the contribution from precursors other than glutamine and direct presynaptic glutamate reuptake cannot maintain the glutamate neurotransmitter pool even during periods of low-frequency activity. A possible explanation for the absence of run down with LFS is that in the acutely isolated brain slice, there is a large
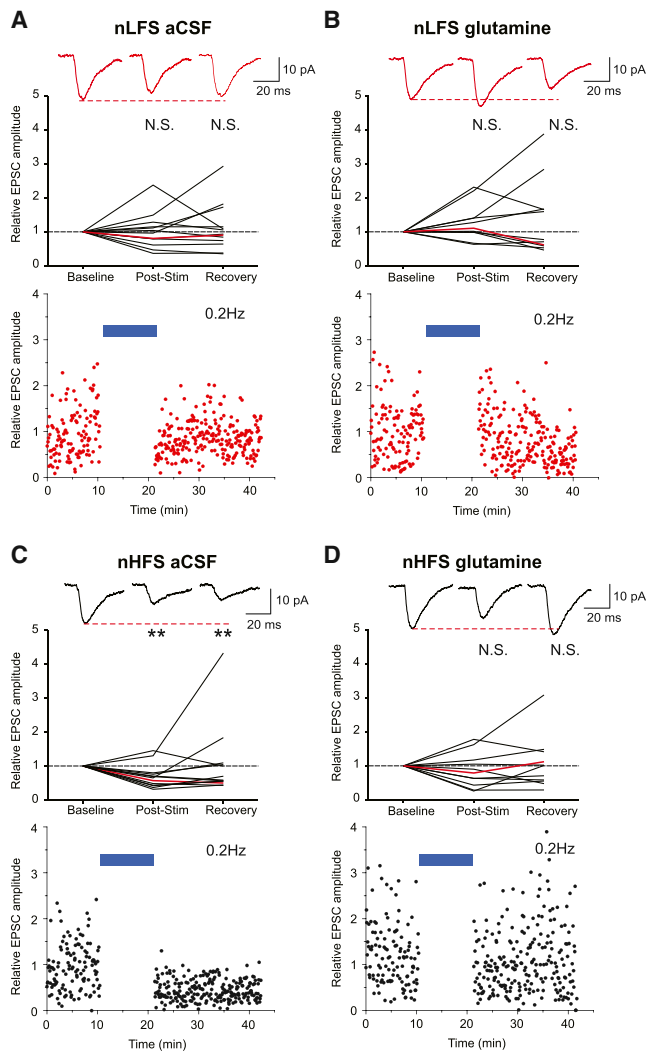
Figure 8. Minimally Evoked Natural Stimulus Pattern Reveals Gluta-mine-Dependent Reduction in Evoked Synaptic EPSCs

EPSC amplitudes were analyzed from intracellular recordings of CA1 cells in which the Schaffer collaterals were minimally stimulated with natural patterns in the absence or presence of glutamine.

(A) Representative example of averaged minimally evoked EPSC amplitudes (upper panel) during 0.2 Hz stimulation from a CA1 cell over 5 min during baseline (left), the first 5 min post-nLFS (middle), and 10–15 min post-nLFS (right). Red dotted line represents mean baseline amplitude. Relative ampli-tudes of evoked EPSCs from 13 individual cells (middle panel) during baseline, the first 5 min post-nLFS (Poststim), and 10–15 min post-nLFS (recovery) are shown. Red continuous line depicts representative median response corre-sponding to the representative traces. Time course of evoked EPSC ampli-tudes from a representative cell normalized to the median of the baseline is shown (bottom panel). Blue bar represents duration of natural stimulus.

(B–D) Same as above but with (B) nLFS in glutamine (n = 11), (C) nHFS in aCSF (n = 13), and (D) nHFS in glutamine (n = 11). A significant reduction of evoked EPSCs was seen with nHFS in aCSF during poststim (0.65 median; **p < 0.05) and recovery (0.58 median; **p < 0.05), but not in glutamine (one-way ANOVA; aCSF p = 0.0134, glutamine p = 0.9125 for difference within groups). There was no significant difference in evoked EPSCs with nLFS with or without glutamine.

glutamate/glutamine reservoir that feeds into the neurotrans-mitter supply. This explanation is supported by our finding that the effect of MSO is only evident after 1,000 stimuli at both 2 and 20 Hz stimulation.

If there is such a large supply of glutamate and glutamine avail-able, is there any role for regulation of the glutamate-glutamine cycle in synaptic plasticity? Reduced synaptic efficacy associ-ated with high-frequency stimulation is a well-established phe-nomenon (Collingridge et al., 2010). The depletion of glutamate available for release that we describe may explain a portion of short-term synaptic depression associated with prolonged high-frequency stimulation (Garcia-Perez et al., 2008; Stevens and Wesseling, 1999; Wesseling and Lo, 2002). Our iHFS para-digm likely creates a neurotransmitter supply demand similar to normal physiological phenomena including bursts of 20–30 Hz oscillations lasting many tens of seconds in the hippo-campi of mice exploring novel environments (Berke et al., 2008; Hermann et al., 2007; Taberner and Liberman, 2005). Inter-estingly, compared to a continuous intense stimulus such as high potassium, intermittent high-frequency activity likely leads to greater amounts of neurotransmitter release because the periods of low-frequency activity allow for recovery of the releas-able vesicle pool that is rapidly depleted during intense stimula-tion (Sara et al., 2002). This may explain, in part, previous reports of sustained excitatory neurotransmission during intense stimu-lation (Kam and Nicoll, 2007; Masson et al., 2006). Furthermore, the high-frequency natural stimulus pattern led to a glutamine-dependent run down in synaptic efficacy that paralleled what we observed with iHFS. The mean firing frequency of the nHFS pattern corresponds to the range of firing rates for place cells in field, whereas the nLFS that did not lead to a run down in effi-cacy corresponds to the low end of activity of place cells in the field (Mizuseki and Buzsáki, 2013) and similar to the average firing rate of CA3 cells recorded during rapid eye movement (REM) sleep (Mizuseki et al., 2012). The level of activity in our nHFS pattern is maintained in vivo much longer than replayed in our experiment, and because these recordings were from rodents running laps in a familiar environment without novel cues, the mean firing frequency in a novel environment may be even greater (Berke et al., 2008).

The mechanisms underlying the reduced synaptic efficacy with neurotransmitter depletion may involve both a reduction in release probability and a reduction in quantal size. The reduction in the amplitude of evoked responses with minimal stimulation after nHFS suggests a reduction in the amount of glutamate release with single synaptic events, consistent with previous findings of reduced synaptic event amplitudes with disruption of the glutamate-glutamine cycle (Bonansco et al., 2011; Tani et al., 2010). Recent work has demonstrated that the recycling vesicle pool size and release probability at GABAergic synapses are reduced when cytosolic neurotransmitter supply is limited (Wang et al., 2013). This is consistent with previous studies of cholinergic synapses (Poulain et al., 1986) and with our find-ings of an increased paired-pulse ratio in MSO-treated slices after iHFS.

Although our data suggest that concentrations of glutamine in CSF provide a buffer, recent findings indicate that high-fre-quency stimulation in vivo can reduce glutamine concentration

at nerve terminals (Jenstad et al., 2009), suggesting that the capacity of the glutamate-glutamine cycle may provide a ceiling for the rate at which glutamate is released at excitatory synapses. The regulation of cycle components including system N transporters and GS may therefore provide a novel mechanism for altering synaptic efficacy in normal and diseased states (Balkrishna et al., 2010; Dai et al., 2012; Nissen-Meyer et al., 2011; Sidoryk-Wegrzynowicz et al., 2011).

EXPERIMENTAL PROCEDURES

Preparation of Brain Slices

Briefly, following all guidelines of Stanford University's Institutional Animal Care and Use Committee, Sprague-Dawley rats (3–8 weeks) were anesthetized (55 mg/kg pentobarbital through intraperitoneal injection), decapitated, and the brains were rapidly removed and placed in chilled (4°C) low-Ca, low-Na^+ slicing solution consisting of 234 mM sucrose, 11 mM glucose, 24 mM $NaHCO_3$, 2.5 mM KCl, 1.25 mM NaH_2PO_4, 10 mM $MgSO_4$, and 0.5 mM $CaCl_2$, equilibrated with a mixture of 95% O_2 and 5% CO_2. The brain was glued to the slicing stage of a Leica VT1200 sectioning system, and slices (350 μm) were cut in a coronal orientation. The slices were then incubated for 1 hr in 32°C oxygenated aCSF consisting of 126 mM NaCl, 26 mM $NaHCO_3$, 3 mM KCl, 1.25 mM NaH_2PO_4, 2 mM $MgCl_2$, 2 mM $CaCl_2$, and 10 mM glucose. For hippocampal slices, a transaction was made between CA1 and CA3 with a scalpel blade while the sectioned brain was in cold cutting solution.

Field Recordings

Hippocampus

Slices were placed in an interface chamber maintained at 32°C–34°C and superfused with oxygenated aCSF at 2 ml/min and stimulated with a concentric bipolar electrode at Schaffer collaterals with 20–100 μA pulses of 100 μs duration at 0.2 Hz (unless otherwise indicated) delivered by a stimulus isolator (World Precision Instruments). Stimulus current was adjusted to induce an FV amplitude of 0.15 mV (±0.05 mV) during the baseline period of the experiment and was maintained at this level throughout the experiment except during I/O curve measurements. The I/O curve was normalized to the highest stimulus intensity tested (0.3 mV FV amplitude). For each slice, two stimulating electrodes were placed on either side of the recording electrode, with slight displacement to ensure stimulation of nonoverlapping parallel Schaffer collateral pathways. Displacement position and stimulus sides were randomly altered between slices. During 0.2 Hz baseline data acquisition, the stimulation of the test (iHFS) pathway was interleaved with the stimulation of the control (no HFS) pathway 2.5 s apart.

Cortex

Slices were placed in an interface chamber with oxygenated aCSF and transected vertically from layer II to the subcortical white matter and then horizontally below layer I on one side of the vertical cut in aCSF with 10 mM Mg. The slice was then superfused with oxygenated aCSF at 2 ml/min with D-APV (50 μM). The isolated layer I fibers were stimulated with a concentric bipolar electrode with 20–100 μA pulses of 100 μs duration at 0.2 Hz, or as indicated.

aCSF contained 50 μM D-APV or 100 μM DL-APV with or without 500 μM glutamine as indicated. For MSO experiments, individual slices were incubated in freshly prepared 5 mM MSO in oxygenated aCSF for 1 hr at room temperature. We have previously shown that this treatment leads to a greater than 75% reduction in glutamine content in the slice (Tani et al., 2010). The slices were then transferred onto the recording rig in indicated aCSF solutions without MSO.

Electrophysiological data were recorded from glass micropipette electrodes ~1 MΩ filled with aCSF using an Axon Multiclamp 700A amplifier and Digidata 1322A digitizer with pClamp software (Molecular Devices). Slices with more than 40% change in FV amplitude during recording were discarded from analysis. Slices were also excluded from analysis if a spreading depression-like event, defined as a concurrent and significant unprovoked change in evoked fEPSPs from both stimulating electrodes, occurred.

Natural Stimulus Pattern

Twelve minutes of in vivo unit recordings from two CA3 pyramidal cells from an adult male Long-Evans rat running laps in a linear track field (as described in Mizuseki et al., 2009) were converted to time-stamped stimulus patterns (100 μs per event), which was then played back as waveform patterns in 100 s segments sequentially in Clampex to drive two stimulators simultaneously while recording from a single recording electrode. Predefined temporal patterns allowed discrimination of nLFS and nHFS postanalysis.

Whole-Cell Recordings

Whole-cell voltage-clamp recordings were made from CA1 pyramidal cells using 2–5 MΩ pipettes filled with a solution containing 120 mM K gluconate, 10 mM HEPES, 11 mM KCl, 1 mM $MgCl_2$, 11 mM EGTA, and 1 mM $CaCl_2$ (pH 7.3). During EPSC recordings, the CA1 cell membrane was clamped at −57.7 mV, and pharmacologically isolated AMPA currents were recorded by bath application of the GABAA receptor antagonist picrotoxin (50 μM; Tocris) and NMDA receptor antagonist (D-APV, 50 μM); access resistance was monitored at the beginning and end of the recordings, and only cells with stable access resistance were included in the analysis. Stimulation setup was the same as for field potential recordings. A modified minimal stimulation approach based on Dobrunz and Stevens (1997) was used. Briefly, pulse pairs (40 ms interval) were applied at 0.2 Hz while adjusting stimulus strength to find conditions of minimal stimulation. The stimulus current was varied until a range of current was found for which three parameters were met: the EPSC amplitude remained constant, failures were observed, and a small reduction in stimulus amplitude resulted in 100% failures. Typically, this range was 10–50 pA.

For evoked EPSCs, a low-pass Gaussian filter was used at 1 kHz to reduce signal-to-noise ratio, and the amplitudes were calculated as the maximum peak-to-baseline value. Values smaller than 5 pA that were indistinguishable from noise were considered failures and were not included in the analysis of evoked EPSC amplitude. Failure rate was assessed and found to be unchanged in each condition (data not shown). Average raw amplitude values in each condition were not significantly different from one another and ranged from 20 to 26 pA. Normality was assessed by performing the Shapiro-Wilk normality test and statistical significance by performing one-way ANOVA or Kruskal-Wallis one-way ANOVA on Ranks.

Biosensor Imaging

Glutamate biosensor data were collected and analyzed as previously described (Dulla et al., 2008). Briefly, 50 μl of FLII81E-1 μM FRET-based glutamate biosensor protein (50 ng/μl) was applied to the slice on a 35 mm culture dish filled with 2 ml aCSF in a humidified chamber. After 10–20 min of incubation, the slice was placed into the recording chamber for simultaneous imaging and electrophysiological recording (Dulla et al., 2008). The slice was illuminated with 440 nm light, and CFP (426–446 nm range) and Venus (505–565 nm range) signals were imaged at 500 Hz with a RedShirt Neuro-CCD camera. Ratiometric glutamate biosensor movies were collected during ten successive stimulations and adjusted for bleaching using an exponential decay and then averaged. From the averaged movie, an integrated glutamate response was generated by summing 30 frames of baseline-subtracted data. The region of biosensor signal change was determined by threshold analysis. Briefly, all pixels with an integrated change in FRET of <0.001 were discarded, and the remaining pixels were ranked based on intensity. The pixels with the 90th–100th percentile most-intense signal were selected, and stray pixels were eliminated using an erosion filter. This region of interest was then used to analyze the FRET ratio for each individual glutamate movie, and the response (ΔFRET ratio) was averaged for all ten movies. In order to generate representative images for each response, the ΔFRET images were blanked outside of the region of interest and overlaid on a bright-field image of the isotopic area.

Drugs and Reagents

All salts and glucose for use in buffers were obtained from Sigma-Aldrich. In addition, the following reagents were also obtained from Sigma-Aldrich: L-MSO (M5379) and L-glutamine (G3126). γ-DGG (ASC-307), D-APV (ASC-003), and DL-APV (ASC-004) were obtained from Ascent Scientific.

Data Analysis

Data recorded by pClamp were analyzed using Clampfit software (Molecular Devices), as well as with in-house software written in MATLAB. Relative changes in fEPSP amplitudes and area were analyzed as indicated.

Statistics

Unless otherwise indicated, statistical significance for all experiments was determined using Student's unpaired and paired t tests as well as ANOVA, as appropriate.

SUPPLEMENTAL INFORMATION

Supplemental Information includes three figures and can be found with this article online at http://dx.doi.org/10.1016/j.neuron.2013.12.026.

REFERENCES

Aoki, C., Kaneko, T., Starr, A., and Pickel, V.M. (1991). Identification of mitochondrial and non-mitochondrial glutaminase within select neurons and glia of rat forebrain by electron microscopic immunocytochemistry. J. Neurosci. Res. 28, 531–548.

Bacci, A., Sancini, G., Verderio, C., Armano, S., Pravettoni, E., Fesce, R., Franceschetti, S., and Matteoli, M. (2002). Block of glutamate-glutamine cycle between astrocytes and neurons inhibits epileptiform activity in hippocampus. J. Neurophysiol. 88, 2302–2310.

Balkrishna, S., Bröer, A., Kingsland, A., and Bröer, S. (2010). Rapid downregulation of the rat glutamine transporter SNAT3 by a caveolin-dependent trafficking mechanism in Xenopus laevis oocytes. Am. J. Physiol. Cell Physiol. 299, C1047–C1057.

Bergles, D.E., and Jahr, C.E. (1998). Glial contribution to glutamate uptake at Schaffer collateral-commissural synapses in the hippocampus. J. Neurosci. 18, 7709–7716.

Berke, J.D., Hetrick, V., Breck, J., and Greene, R.W. (2008). Transient 23-30 Hz oscillations in mouse hippocampus during exploration of novel environments. Hippocampus 18, 519–529.

Billups, D., Marx, M.-C., Mela, I., and Billups, B. (2013). Inducible presynaptic glutamine transport supports glutamatergic transmission at the calyx of Held synapse. J. Neurosci. 33, 17429–17434.

Bonansco, C., Couve, A., Perea, G., Ferradas, C.A., Roncagliolo, M., and Fuenzalida, M. (2011). Glutamate released spontaneously from astrocytes sets the threshold for synaptic plasticity. Eur. J. Neurosci. 33, 1483–1492.

Boulland, J.L., Osen, K.K., Levy, L.M., Danbolt, N.C., Edwards, R.H., Storm-Mathisen, J., and Chaudhry, F.A. (2002). Cell-specific expression of the glutamine transporter SN1 suggests differences in dependence on the glutamine cycle. Eur. J. Neurosci. 15, 1615–1631.

Branco, T., and Staras, K. (2009). The probability of neurotransmitter release: variability and feedback control at single synapses. Nat. Rev. Neurosci. 10, 373–383.

Bushong, E.A., Martone, M.E., Jones, Y.Z., and Ellisman, M.H. (2002). Protoplasmic astrocytes in CA1 stratum radiatum occupy separate anatomical domains. J. Neurosci. 22, 183–192.

Cauller, L.J., and Connors, B.W. (1994). Synaptic physiology of horizontal afferents to layer I in slices of rat SI neocortex. J. Neurosci. 14, 751–762.

Christie, J.M., and Jahr, C.E. (2006). Multivesicular release at Schaffer collateral-CA1 hippocampal synapses. J. Neurosci. 26, 210–216.

Collingridge, G.L., Peineau, S., Howland, J.G., and Wang, Y.T. (2010). Long-term depression in the CNS. Nat. Rev. Neurosci. 11, 459–473.

Dai, M., Xia, X.B., and Xiong, S.Q. (2012). BDNF regulates GLAST and glutamine synthetase in mouse retinal Müller cells. J. Cell. Physiol. 227, 596–603.

Danbolt, N.C. (2001). Glutamate uptake. Prog. Neurobiol. 65, 1–105.

Dobrunz, L.E., and Stevens, C.F. (1997). Heterogeneity of release probability, facilitation, and depletion at central synapses. Neuron 18, 995–1008.

Dulla, C., Tani, H., Okumoto, S., Frommer, W.B., Reimer, R.J., and Huguenard, J.R. (2008). Imaging of glutamate in brain slices using FRET sensors. J. Neurosci. Methods 168, 306–319.

Dulla, C.G., Tani, H., Brill, J., Reimer, R.J., and Huguenard, J.R. (2012). Glutamate biosensor imaging reveals dysregulation of glutamatergic pathways in a model of developmental cortical malformation. Neurobiol. Dis. 49C, 232–246.

Fricke, M.N., Jones-Davis, D.M., and Mathews, G.C. (2007). Glutamine uptake by System A transporters maintains neurotransmitter GABA synthesis and inhibitory synaptic transmission. J. Neurochem. 102, 1895–1904.

Furness, D.N., Dehnes, Y., Akhtar, A.Q., Rossi, D.J., Hamann, M., Grutle, N.J., Gundersen, V., Holmseth, S., Lehre, K.P., Ullensvang, K., et al. (2008). A quantitative assessment of glutamate uptake into hippocampal synaptic terminals and astrocytes: new insights into a neuronal role for excitatory amino acid transporter 2 (EAAT2). Neuroscience 157, 80–94.

Garcia-Perez, E., Lo, D.C., and Wesseling, J.F. (2008). Kinetic isolation of a slowly recovering component of short-term depression during exhaustive use at excitatory hippocampal synapses. J. Neurophysiol. 100, 781–795.

Gundersen, V., Danbolt, N.C., Ottersen, O.P., and Storm-Mathisen, J. (1993). Demonstration of glutamate/aspartate uptake activity in nerve endings by use of antibodies recognizing exogenous D-aspartate. Neuroscience 57, 97–111.

Halassa, M.M., Fellin, T., Takano, H., Dong, J.H., and Haydon, P.G. (2007). Synaptic islands defined by the territory of a single astrocyte. J. Neurosci. 27, 6473–6477.

Hanse, E., and Gustafsson, B. (2001). Paired-pulse plasticity at the single release site level: an experimental and computational study. J. Neurosci. 21, 8362–8369.

Hermann, J., Pecka, M., von Gersdorff, H., Grothe, B., and Klug, A. (2007). Synaptic transmission at the calyx of Held under in vivo like activity levels. J. Neurophysiol. 98, 807–820.

Hertz, L. (1979). Functional interactions between neurons and astrocytes I. Turnover and metabolism of putative amino acid transmitters. Prog. Neurobiol. 13, 277–323.

Jenstad, M., Quazi, A.Z., Zilberter, M., Haglerød, C., Berghuis, P., Saddique, N., Goiny, M., Buntup, D., Davanger, S., S Haug, F.M., et al. (2009). System A transporter SAT2 mediates replenishment of dendritic glutamate pools controlling retrograde signaling by glutamate. Cereb. Cortex 19, 1092–1106.

Kam, K., and Nicoll, R. (2007). Excitatory synaptic transmission persists independently of the glutamate-glutamine cycle. J. Neurosci. 27, 9192–9200.

Keyser, D.O., and Pellmar, T.C. (1994). Synaptic transmission in the hippocampus: critical role for glial cells. Glia 10, 237–243.

Kvamme, E. (1998). Synthesis of glutamate and its regulation. Prog. Brain Res. 116, 73–85.

Liang, S.L., Carlson, G.C., and Coulter, D.A. (2006). Dynamic regulation of synaptic GABA release by the glutamate-glutamine cycle in hippocampal area CA1. J. Neurosci. 26, 8537–8548.

Lieth, E., LaNoue, K.F., Berkich, D.A., Xu, B., Ratz, M., Taylor, C., and Hutson, S.M. (2001). Nitrogen shuttling between neurons and glial cells during glutamate synthesis. J. Neurochem. 76, 1712–1723.

Liu, G., Choi, S., and Tsien, R.W. (1999). Variability of neurotransmitter concentration and nonsaturation of postsynaptic AMPA receptors at synapses in hippocampal cultures and slices. Neuron 22, 395–409.

Masson, J., Darmon, M., Conjard, A., Chuhma, N., Ropert, N., Thoby-Brisson, M., Foutz, A.S., Parrot, S., Miller, G.M., Jorisch, R., et al. (2006). Mice lacking brain/kidney phosphate-activated glutaminase have impaired glutamatergic synaptic transmission, altered breathing, disorganized goal-directed behavior and die shortly after birth. J. Neurosci. 26, 4660–4671.

Mizuseki, K., and Buzsáki, G. (2013). Preconfigured, skewed distribution of firing rates in the hippocampus and entorhinal cortex. Cell Rep. 4, 1010–1021.

Mizuseki, K., Sirota, A., Pastalkova, E., and Buzsáki, G. (2009). Theta oscillations provide temporal windows for local circuit computation in the entorhinal-hippocampal loop. Neuron 64, 267–280.

Mizuseki, K., Royer, S., Diba, K., and Buzsáki, G. (2012). Activity dynamics and behavioral correlates of CA3 and CA1 hippocampal pyramidal neurons. Hippocampus 22, 1659–1680.

Moore, J.J., Sax, S.M., and Blackburn, A.B., Jr. (1978). Determination of spinal fluid glutamine with the Du Pont aca. Clin. Chem. 24, 2213–2214.

Nissen-Meyer, L.S., Popescu, M.C., Hamdani el, H., and Chaudhry, F.A. (2011). Protein kinase C-mediated phosphorylation of a single serine residue on the rat glial glutamine transporter SN1 governs its membrane trafficking. J. Neurosci. 31, 6565–6575.

Otsuki, T., Nakama, H., Kanamatsu, T., and Tsukada, Y. (2005). Glutamate metabolism in epilepsy: 13C-magnetic resonance spectroscopy observation in the human brain. Neuroreport 16, 2057–2060.

Poulain, B., Baux, G., and Tauc, L. (1986). Presynaptic transmitter content controls the number of quanta released at a neuro-neuronal cholinergic synapse. Proc. Natl. Acad. Sci. USA 83, 170–173.

Rothman, D.L., Behar, K.L., Hyder, F., and Shulman, R.G. (2003). In vivo NMR studies of the glutamate neurotransmitter flux and neuroenergetics: implications for brain function. Annu. Rev. Physiol. 65, 401–427.

Sara, Y., Mozhayeva, M.G., Liu, X., and Kavalali, E.T. (2002). Fast vesicle recycling supports neurotransmission during sustained stimulation at hippocampal synapses. J. Neurosci. 22, 1608–1617.

Schousboe, A., Westergaard, N., Sonnewald, U., Petersen, S.B., Huang, R., Peng, L., and Hertz, L. (1993). Glutamate and glutamine metabolism and compartmentation in astrocytes. Dev. Neurosci. 15, 359–366.

Sibson, N.R., Mason, G.F., Shen, J., Cline, G.W., Herskovits, A.Z., Wall, J.E., Behar, K.L., Rothman, D.L., and Shulman, R.G. (2001). In vivo (13)C NMR measurement of neurotransmitter glutamate cycling, anaplerosis and TCA cycle flux in rat brain during. J. Neurochem. 76, 975–989.

Sidoryk-Wegrzynowicz, M., Lee, E., Mingwei, N., and Aschner, M. (2011). Disruption of astrocytic glutamine turnover by manganese is mediated by the protein kinase C pathway. Glia 59, 1732–1743.

Stevens, C.F., and Wesseling, J.F. (1999). Identification of a novel process limiting the rate of synaptic vesicle cycling at hippocampal synapses. Neuron 24, 1017–1028.

Taberner, A.M., and Liberman, M.C. (2005). Response properties of single auditory nerve fibers in the mouse. J. Neurophysiol. 93, 557–569.

Tani, H., Dulla, C.G., Huguenard, J.R., and Reimer, R.J. (2010). Glutamine is required for persistent epileptiform activity in the disinhibited neocortical brain slice. J. Neurosci. 30, 1288–1300.

Uwechue, N.M., Marx, M.C., Chevy, Q., and Billups, B. (2012). Activation of glutamate transport evokes rapid glutamine release from perisynaptic astrocytes. J. Physiol. 590, 2317–2331.

Wang, L., Tu, P., Bonet, L., Aubrey, K.R., and Supplisson, S. (2013). Cytosolic transmitter concentration regulates vesicle cycling at hippocampal GABAergic terminals. Neuron 80, 143–158.

Wesseling, J.F., and Lo, D.C. (2002). Limit on the role of activity in controlling the release-ready supply of synaptic vesicles. J. Neurosci. 22, 9708–9720.